

Precipitation Processing System (PPS)



NASA Global Precipitation Measurement (GPM) Microwave Imager (GMI) Level 1B (L1B) Algorithm Theoretical Basis Document (ATBD)

Prepared By:

NATIONAL AERONAUTICS AND SPACE ADMINISTRATION
GODDARD SPACE FLIGHT CENTER
Code 610.2/PPS
Greenbelt, Maryland 20771

November 2010

Goddard Space Flight Center
Greenbelt, Maryland



National Aeronautics and
Space Administration

TABLE OF CONTENTS

1.0 INTRODUCTION.....	1-1
1.1 OBJECTIVE	1-1
1.2 INSTRUMENT DESCRIPTION.....	1-1
1.3 L1B ALGORITHM OVERVIEW.....	1-3
1.4 L1B DATA DESCRIPTION	1-4
2.0 GEOLOCATION ALGORITHM	2-1
3.0 CALIBRATION ALGORITHM	3-1
3.1 RADIOMETRIC CALIBRATION.....	3-1
3.1.1 Non-Linear Radiometric Calibration	3-2
3.1.2 Hot Load View.....	3-2
3.1.3 Cold Sky View.....	3-4
3.1.4 Earth View	3-5
3.1.5 Noise Diodes and Four-Point Calibration.....	3-7
3.1.6 Back-up Calibration Algorithm	3-8
3.2 ANTENNA PATTERN CORRECTION.....	3-8
3.3 INPUT, OUTPUT, AND ALGORITHM FLOW CHART	3-8
3.4 PRE-LAUNCH SIMULATION AND SYNTHETIC L1B DATA.....	3-10
3.5 POST-LAUNCH VALIDATION AND CALIBRATION	3-14
3.5.1 Pointing Error Check	3-14
3.5.2 Along-Scan Correction	3-15
3.5.3 Inter-Comparison and Statistical Analysis.....	3-15
3.5.4 Deep-Space Maneuver	3-15
4.0 L1B DATA PRODUCT	4-1
4.1 LEVEL 1B PROCESSING	4-1
4.1.1 Satellite Maneuver	4-1
4.1.2 GMI L1B Processing	4-1
4.2 DATA STRUCTURE.....	4-2
4.2.1 Metadata.....	4-3
4.2.2 Structure	4-3
5.0 REFERENCES.....	5-1
APPENDIX A. ACRONYMS AND ABBREVIATIONS.....	A-1

LIST OF TABLES

Table 1-1. Reference for Important Instrument and Orbital Parameters.....	1-3
Table 3-1. Key Input Parameters.....	3-9
Table 3-2. Comparison of Channel Characteristics Between GMI and Existing Satellite Sensors.....	3-11

LIST OF FIGURES

Figure 1-1. GMI Instrument Stowed Configuration.....	1-1
Figure 1-2. GMI Instrument Deployed Configuration.....	1-2
Figure 1-3. Top-Level Flow Chart of the GMI L1B Algorithm.....	1-4
Figure 3-1. Calibration Assembly Configuration.....	3-1
Figure 3-2. Schematic Diagram of GMI Three-Point Non-Linear Calibration.....	3-2
Figure 3-3. GMI Hot Load.....	3-3
Figure 3-4. GMI Hot Load PRT Locations.....	3-4
Figure 3-5. Simulated 5-Minute Section of 37 GHz Channel T_b (Upper) and 18 ± 3 GHz T_b (Lower).....	3-6
Figure 3-6. Schematic Diagram of GMI Four-Point Calibration.....	3-7
Figure 3-7. Flow Chart of GMI L1B Calibration Process.....	3-10
Figure 3-8. Flow Diagram of Derivation of Synthetic GMI T_b	3-11
Figure 3-9. T_b Relationships Between GMI 36.5 GHz and TMI 37.0 GHz Channels and Between GMI 89 GHz and TMI 85.5 GHz Channels.....	3-12
Figure 3-10. Global GMI T_b Database for Northern Summer.....	3-13
Figure 3-11. Synthetic Orbital GMI T_b for June 15, 2008.....	3-13
Figure 3-12. Flow Diagram of Synthetic Data Processing.....	3-14
Figure 4-1. Flow Chart for Executing the L1B Main Program and Scan-by-Scan Processing.....	4-2

1.0 INTRODUCTION

1.1 OBJECTIVE

This document describes the GMI Level 1B algorithm. It consists of physical bases and mathematical equations for GMI calibration, as well as pre-launch and post-launch activities. The document also presents high-level software design. However, detailed software descriptions will be presented separately in the Level 1B Software Design Document. Parts of this document are from the RSS GMI Calibration ATBD as contributed by the Ball Aerospace GMI manufactory contract. The GMI L1B geolocation algorithm is described in a separate Geolocation Toolkit (GeoTK) ATBD.

1.2 INSTRUMENT DESCRIPTION

GMI is a primary microwave sensor onboard both the GPM core satellite and constellation satellites. The core satellite flies in a 407-km circular orbit with a 65° inclination angle. The constellation will be a Sun-synchronous (TBD) satellite flying at altitudes of about 635 km. The GMI has 13 channels with a frequency range from 10 GHz to 183 GHz. Except for the heritage hot load and cold load that are commonly used for linear sensor radiometric calibrations, a hot noise diode and a cold noise diode are implemented in the GMI to determine the non-linearity and noise levels of the measurements. Figure 1-1 and Figure 1-2 show the main components of the GMI.

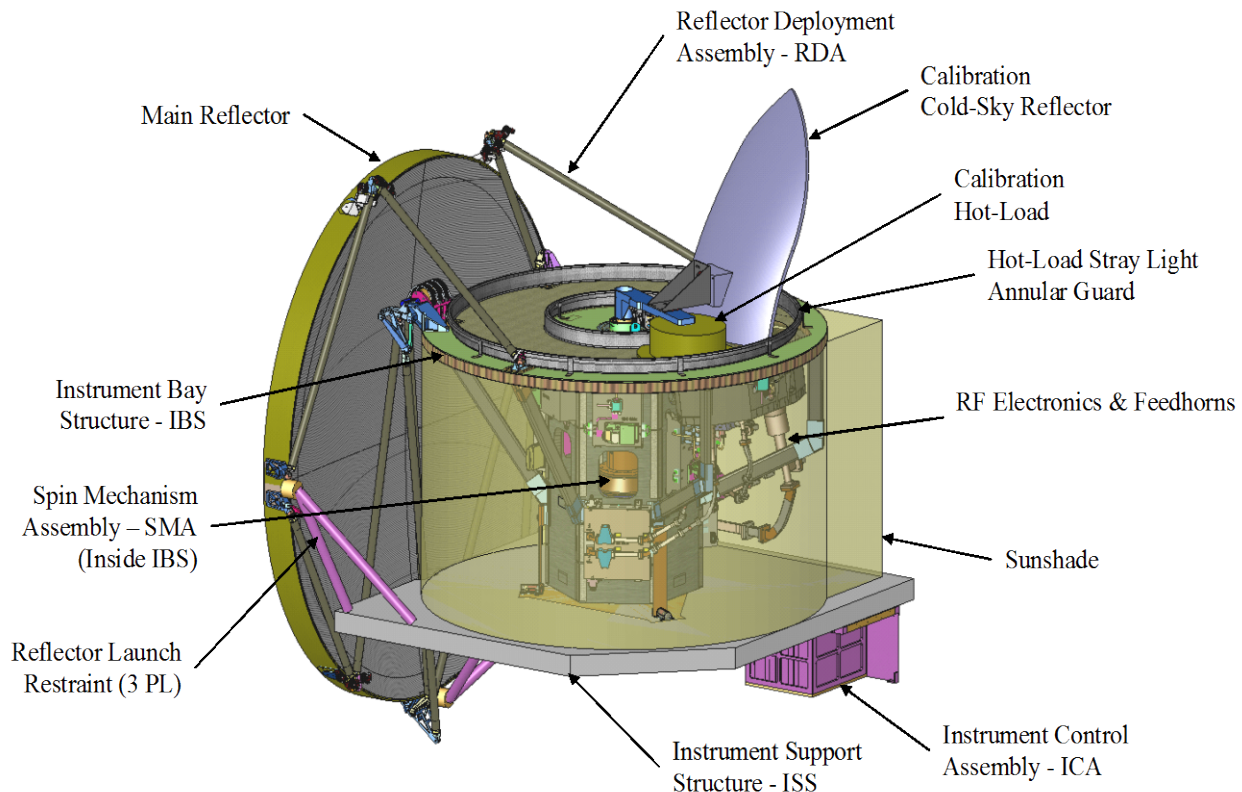


Figure 1-1. GMI Instrument Stowed Configuration
(Provided by Ball Aerospace Corp.)

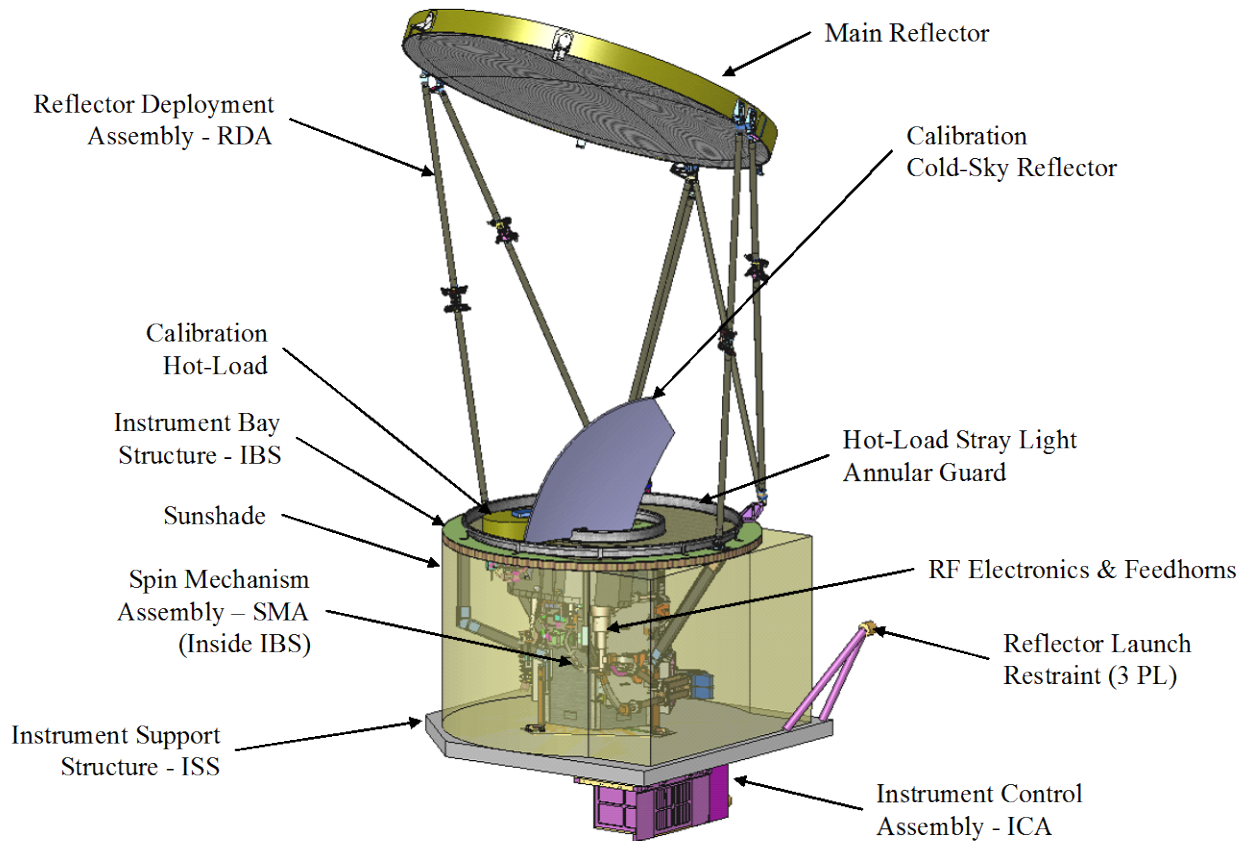


Figure 1-2. GMI Instrument Deployed Configuration
(Provided by Ball Aerospace Corp.)

The GMI sensor data include the following:

- Nominal altitude: 407 km.
- Orbital inclination: 65 deg.
- Spin rate: 32 rpm.
- Scan time: 1.875 sec.
- Swath width: 885 km.
- Earth viewing sector: 140 deg.
- Earth samples: 202.
- Integration time: $3.6 \text{ msec} = (140/360) \times 1.875 \text{ sec}/202$.
- Dish size: 1.22 m.

Some important sensor specifications are cited in Table 1-1.

Table 1-1. Reference for Important Instrument and Orbital Parameters

Chan. #	Center Freq (GHz)	Pass- band Band- width (MHz)	Pol.	Sam- pling Inter- val (ms)	Nadir Angle [deg]	Nominal Earth Inci- dence Angle	Beam Width [deg]	Foot- print [km x km]	Earth Sam- ples per Scan	Cold Sam- ples per Scan	Hot Sam- ples per Scan	NEDT (K) Max
1	10.65	100	V	3.6	48.5	52.821	1.732	32.1× 19.4	202	4	4	0.96
2	10.65	100	H	3.6	48.5	52.821	1.732	32.1× 10.9	202	4	4	0.96
3	18.70	200	V	3.6	48.5	52.821	0.977	18.1× 10.9	202	4	9	0.84
4	18.70	200	H	3.6	48.5	52.821	0.977	18.1× 10.9	202	4	9	0.84
5	23.80	400	V	3.6	48.5	52.821	0.862	16.0× 9.7	202	4	9	1.05
6	36.50	1000	V	3.6	48.5	52.821	0.843	15.6× 9.4	202	9	20	0.65
7	36.50	1000	H	3.6	48.5	52.821	0.843	15.6× 9.4	202	9	20	0.65
8	89.00	6000	V	3.6	48.5	52.821	0.390	7.2 × 4.4	202	9	30	0.57
9	89.00	6000	H	3.6	48.5	52.821	0.390	7.2 × 4.4	202	9	30	0.57
10	166.00	4000	V	3.6	45.36	49.195	0.396	6.3 × 4.1	202	9	25	1.50
11	166.00	4000	H	3.6	45.36	49.195	0.396	6.3 × 4.1	202	9	25	1.50
12	183.31 ± 3.0	2000	V	3.6	45.36	49.195	0.361	5.8 × 3.8	202	9	25	1.50
13	183.31 ± 7.0	2000	V	3.6	45.36	49.195	0.361	5.8 × 3.8	202	9	25	1.50

1.3 L1B ALGORITHM OVERVIEW

The Level 1B algorithm and software transform Level 0 counts into geolocated and calibrated antenna temperatures (T_a) and brightness temperatures (T_b). The T_a is obtained by utilizing the sensor radiometric calibration. The T_b commonly used for generating higher level science data are derived from T_a after antenna pattern correction (APC) and vicarious calibrations. The regular Level 1B process is composed of the following four components: 1) combined geolocation algorithm, 2) GMI sensor radiometric calibration (T_a), 3) APC and vicarious calibration (T_b), and 4) quality assurance (QA).

Figure 1-3 describes the relationship between algorithm components and products (or output).

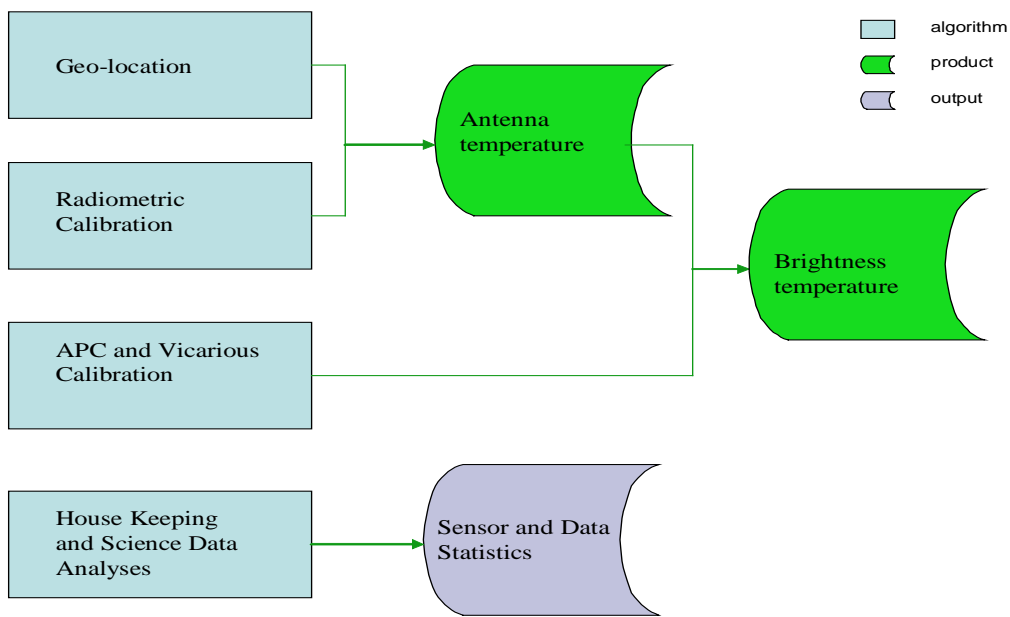


Figure 1-3. Top-Level Flow Chart of the GMI L1B Algorithm

1.4 L1B DATA DESCRIPTION

The standard Level 1B GMI data are geolocated and calibrated microwave antenna temperatures (T_a) and brightness temperatures (T_b) in two separate data files. The base T_a data file will include all calibration parameters and measurements that are used to generate T_a and all navigation parameters that are used to “geolocate” each pixel. The T_b data file will include all parameters for corrections of T_a . Standard L1B data will be in the format of a full orbit (about 90 minutes). Real-time L1B data will be processed in a 10-minute time period.

2.0 GEOLOCATION ALGORITHM

GMI geolocation will be computed using the GMI Geolocation Toolkit (GeoTK). The geolocation algorithm is described in the GeoTK ATBD (Bilanow, 2010). This section gives a brief overview of that algorithm and describes how the inputs to GeoTK are prepared by the L1B algorithm. The purpose of GeoTK is to compute pixel latitude and longitude and various geometric ancillary data (e.g., incidence and Sun angles). Inputs needed from the GMI L1B algorithm provide the direction vectors viewed by the instrument in instrument coordinates and their precise timing. File inputs used by GeoTK include the onboard attitude (i.e., the orientation or pointing) and ephemeris (i.e., position in the orbit) of the GPM spacecraft as extracted from telemetry and processed by the Geo File Builder. Parameter file inputs include information on the alignment of the instrument on the spacecraft and various limit checks to be used for quality assurance. One file output from GeoTK provides QA information that is collected by the PPS processing system for a mission record of geolocation QA data. Details of the inputs and outputs are provided in the PPS Geolocation Toolkit Architecture and Design Specification, PPS 610.2 P520 (Bilanow, 2010).

The basic geometrical model for GMI instrument viewing direction for each channel is based on a conical scan at a constant spin rate. The instrument is assumed to rotate about the +Z axis, and the reference axis from which rotation angles are defined will be the +X axis. The parameters input to this model, derived from spacecraft telemetry, are defined as follows.

Tref = Reference time for when science sampling starts.

Aref = Angle of rotation when science sampling starts.

Tstep = Time between pixel samples (nominally 3.0 milliseconds).

Wrate = Angular spin rate (nominally 32 rpm).

c = Scan cone angular radius (nominally 131.5 degrees).

Thus, the time that each pixel, i , is sampled (starting from index 0) is:

$$t_i = Tref + i * Tstep$$

The rotation angles, a , at which each pixel, i , is sampled are:

$$a_i = Aref + Wrate * (i * Tstep)$$

The viewing direction vector is given by:

$$\text{viewing vector, } \mathbf{V}_i = \begin{bmatrix} \sin(c) \cos(a_i) \\ \sin(c) \sin(a_i) \\ \cos(c) \end{bmatrix}$$

The GeoTK subroutines will return error codes to the upper-level routines. In cases where valid data cannot be computed, fill data are provided. The error handling, in terms of providing error messages to the system operator and terminating processing, will be handled in the calling routines, i.e., the Level 1B processing routines.

3.0 CALIBRATION ALGORITHM

3.1 RADIOMETRIC CALIBRATION

The GMI sensor spins continuously. In each complete rotation, the sensor measures Earth radiation in a section of 140 degrees. Beyond 140 degree up to 145 degrees, the sensor may also take valid Earth measurements if applicable. The other section of the rotation is used for calibration. Operational GMI has a calibration cycle that repeats every two-scan rotation. In the first scan rotation, noise diodes are turned off and the cold sky and the hot load are sampled for the purpose of radiometric calibration. In the second rotation, noise diodes are turned on and the cold sky plus noise diode and hot load plus noise diode are sampled for 10-37 GHz channels. The two-scan calibration cycle provides four calibration points to calculate not only the gain and offset of the receivers, but also the excess noise temperature of the noise diodes and the nonlinearity of the receivers. The calibration assembly configuration is shown in Figure 3-1. Cold sky reflector and hot load are stationary; i.e., they do not rotate with the instrument. The hot load tray mounts to the deck and rotates with the instrument.

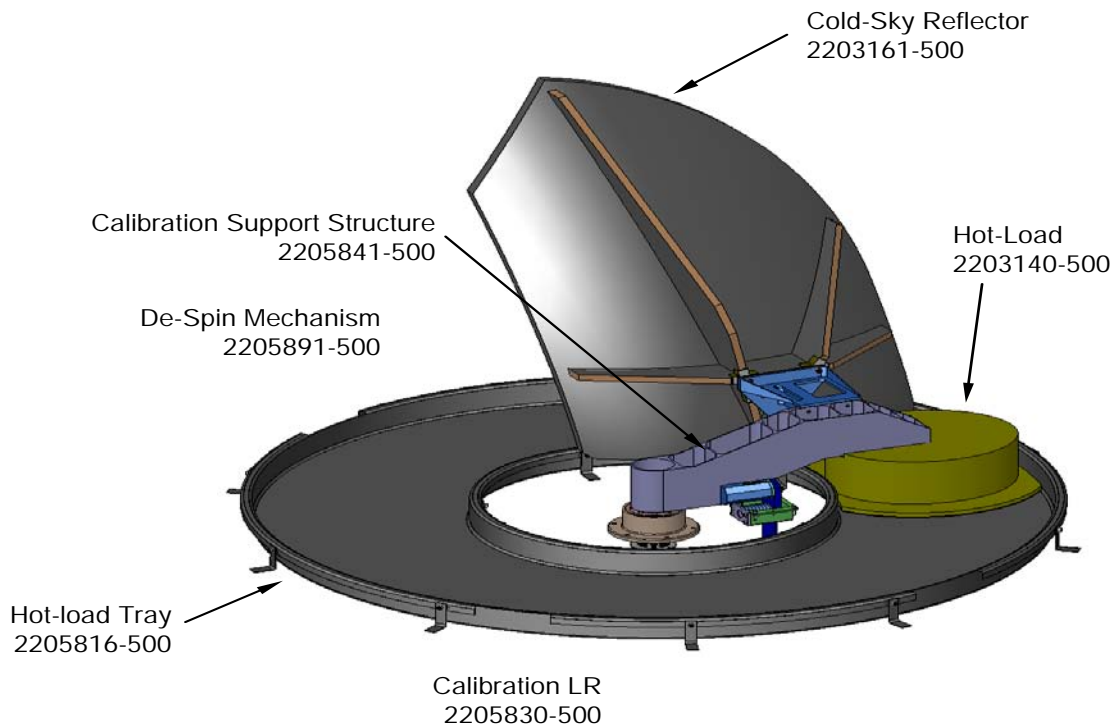


Figure 3-1. Calibration Assembly Configuration
(Taken from GMI Preliminary Design Review [PDR] Days 4-5: Calibration Assembly)

The GMI will use a non-linear three-point in-flight calibration to derive antenna temperature (T_a). The four-point calibration will be used to monitor the sensor non-linearity and to calibrate when hot load measurements are not available.

3.1.1 Non-Linear Radiometric Calibration

If the transfer function were perfectly linear, then two calibration points (hot and cold loads) would uniquely determine the state of the Earth observation. While the goal is to provide receivers that are linear, in reality they are slightly nonlinear. To account for the nonlinearity, a quadratic radiometric transfer function will be used. The quadratic term will be computed from pre-launch data and receiver temperature. Figure 3-2 shows a schematic diagram of the GMI non-linear three-point calibration approach.

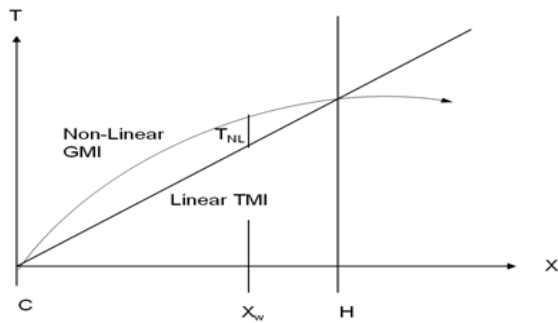


Figure 3-2. Schematic Diagram of GMI Non-Linear Three-Point Calibration

Equation (3.1) shows the GMI non-linear calibration equation for each of the 13 GMI channels:

$$T_{a,i} = X_i * T_h + (1-X_i) * T_c - 4 * T_{nl} * X_i * (1-X_i) \quad (3.1)$$

Where:

$T_{a,i}$: Antenna temperature of each pixel $i = 1, N_{pixel}$.

T_h : Mean hot load temperature; T_c : Mean cold sky temperature.

T_{nl} : Peak non-linearity generated from receiver temperature or from four-point calibration.

$X_i = (C_i - C_c) / (C_h - C_c)$: Radiometer response.

C_i : Earth view count of the pixel; C_c : Mean cold load count; C_h : Mean hot load count.

The calibration equation is applied scan by scan, although multi-scan calibration information may be used.

The nonlinearity will also be calculated on-orbit by the four-point calibration method. If nonlinearity drifts a statistically significant amount, the data can be updated on-orbit. An along-scan correction will be applied to $T_{a,i}$.

3.1.2 Hot Load View

The hot load consists of a non-rotating calibration target that intercepts the line of sight between the feed horns and the main reflector as the feed horns pass beneath the hot calibration load during each scan. The temperature of the hot load is passively controlled and will be between

240 K and 330 K over all on-orbit conditions. The hot load is approximately an elliptical shape with two lobes on one side. It is made up of pyramidal-shaped metal structures coated with an absorbing material called ECCOSORB. Figure 3-3 shows the GMI hot load calibration target. The pyramids are about 0.5" square by about 2.7" tall. The thickness of the base limits the temperature gradients across the load, and the pyramid design in concert with the ECCOSORB allows the emissivity to be ~ 1.0. The load was sized to allow a minimum of four measurements per view for all channels. The hot load will be sampled multiple times per rotation of the main reflector and multiple rotations to minimize the effect of thermal noise.

The emissivity of the hot load is required to be greater than 0.9992 for 10-89 GHz and greater than 0.9999 for 165.5 GHz and 183.3 GHz. The hot load is highly isolated to limit temporal changes in the brightness temperature. At least 11 thermistors (PRTs) are embedded in the hot load and will be available during on-orbit operations. All PRTs are located in the pyramids to lower the temperature uncertainty between the PRTs and the surface of the ECCOSORB coating. The PRTs are also located along the arcs traversed by the feed horns to limit the impact of gradients.

At certain points in the orbit or at certain times, Sun light may hit the hot load and cause additional gradients that cause its effective temperature to deviate from what the PRTs read. The GMI hot load is designed to minimize this effect. However, it will still need to be analyzed during the post-launch calibration and validation.

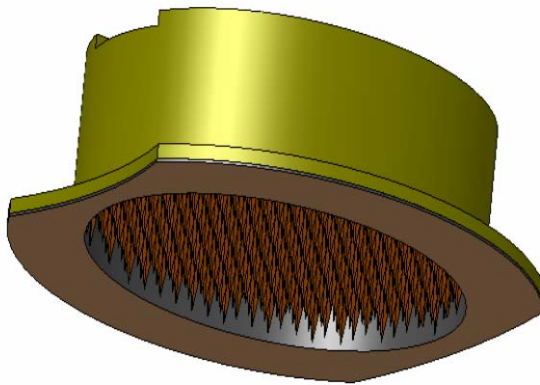


Figure 3-3. GMI Hot Load
 (Taken from GMI PDR Days 4-5: Calibration Assembly) (Randy Keller)

The mean hot load temperature for scan number n will be determined by the following equation:

$$T_h = \frac{\sum_{i=n-na}^{i=n+na} \sum_{j=1}^{j=nt} Wh(i,j) Thot(i,j)}{\sum_{i=n-na}^{i=n+na} \sum_{j=1}^{j=nt} Wh(i,j)} \quad (3.2)$$

Where n is the number of the scan to be calibrated, Thot (i, j) is the hot load temperature taken by thermistor #j measured at scan i. The total number of thermistors nt = 13. The na is the number of scans before and after the current scan (n) that are sampled to calibrate the current scan. However, the sampling takes only every other scan for channels 1-7 when the noise diodes are turned off.

Wh (i, j) is the weighting function to determine if the hot load temperature is valid and the weighting value if valid. The out-of-bound check will be performed to each Wh (i, j). The mean hot load count is determined by Equation (3.3):

$$C_h = \frac{(\sum_{i=n-na}^{i=n+na} \sum_{k=1}^{k=ns} Whc(i, k) Chot(i, k))}{(\sum_{i=n-na}^{i=n+na} \sum_{k=1}^{k=ns} Whc(i, k))} \quad (3.3)$$

$Chot(i, k)$ is the hot load count from sample k at scan i. ns is the total number of hot load sampling listed in Table 1-1. $Whc(i, k)$ is the weighting function for hot load count. Solar correction and out-of-bound check are performed for each $Chot(i, k)$.

The hot load PRTs are located along two tracks that the feeds follow (Figure 3-4). Therefore, the weighting function will be different for channels 1-9 and 10-13.

Hot Load PRT Locations

- Hot Load PRTs are located along two tracks that the feeds follow

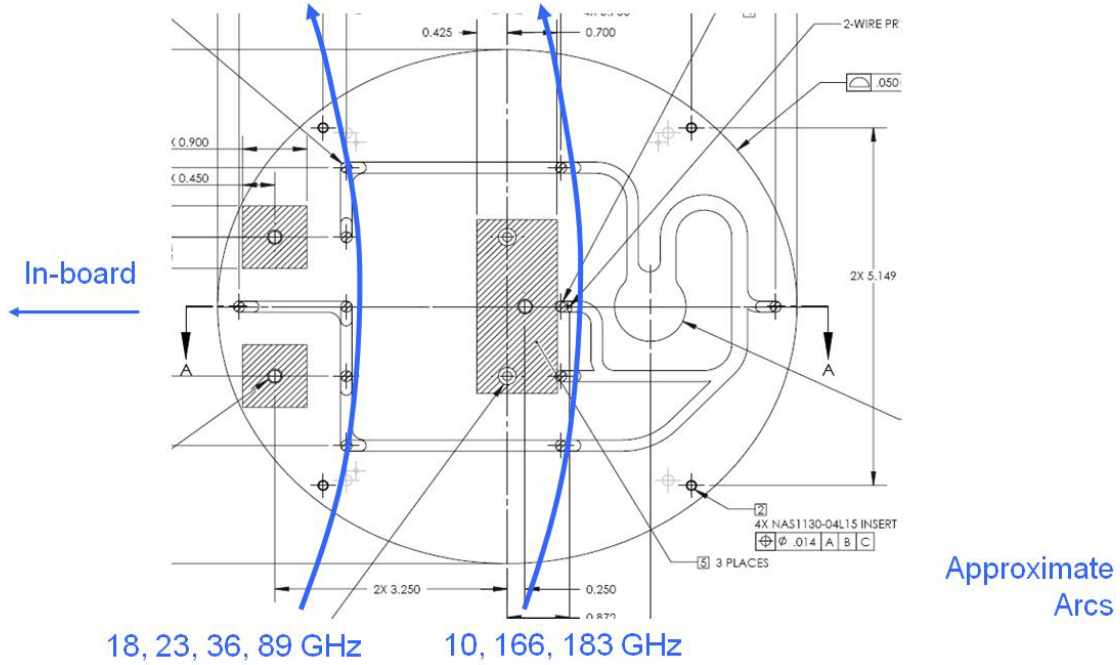


Figure 3-4. GMI Hot Load PRT Locations

3.1.3 Cold Sky View

The cold calibration point is provided by the cold sky reflector (CSR), which allows the feed horns to view targets with a temperature of approximately 2.7 K. The cold sky view is also sampled multiple times per rotation of the main reflector and over multiple rotations of the main reflector. The cold sky view is a more complex combination of sources than the hot load. Contributions other than those from cold space come from reflections and emission from the instrument. There is also Earth view intrusion into the cold sky view primarily through the back lobe of the CSR. The back lobe examines the main reflector, which detects the Earth. The CSR is tilted up at a sufficient angle such that little contamination comes from the Earth directly.

Due to the orbital and cold sky view geometry, the Moon may intrude into the cold sky view. This lunar intrusion has been clearly observed in many other satellite microwave radiometers that employ cold sky calibration (SSM/I, SSMIS, TMI, AMSR, and WindSat). The calibration algorithm will remove as much of the contamination of the cold sky view as possible. Equation (3.4) is used to calculate mean cold sky temperature T_c :

$$T_c = \frac{(\sum_{i=n-na}^{i=n+na} \sum_{j=1}^{j=nt} Wc(i,j) T_{cold}(i,j))}{(\sum_{i=n-na}^{i=n+na} \sum_{j=1}^{j=nt} Wc(i,j))} \quad (3.4)$$

Where n is the number of the scan to be calibrated, $T_{cold}(i, j)$ is the cold sky temperature. The base $T_{cold}(i, j)$ is 2.7 K. It is adjusted by a number of factors such as CSR temperature, CSR emissivity, Earth location, Earth temperature, Earth beam fraction, etc. nt may be greater than 1 if the adjusted cold sky temperature varies along a scan. na is the number of scans before and after the current scan (n) that are sampled to calibrate the current scan. $Wc(i, j)$ is the weighting function to determine if the cold sky temperature is valid and the weighting value if valid.

The mean cold sky count is determined by Equation (3.5):

$$C_c = \frac{(\sum_{i=n-na}^{i=n+na} \sum_{k=1}^{k=ns} Wcc(i,k) C_{cold}(i,k))}{(\sum_{i=n-na}^{i=n+na} \sum_{k=1}^{k=ns} Wcc(i,k))} \quad (3.5)$$

$C_{cold}(i, k)$ is the cold load count from sample k at scan i. ns is the total number of cold load sampling listed in Table 1-1. $Wcc(i, k)$ is the weighting function for cold load count. Moon correction and out-of-bound check are performed for each $C_{cold}(i, k)$.

3.1.4 Earth View

A forward section about 140° is used to view the Earth targets. The normal data have 202 samples in each scan. However, in cases when the data beyond 140° are useful, one scan may have more than 202 pixels. Due to the difference of incidence angles between lower frequency (channels 1-9) and higher frequency (channels 10-13) channels, the swath widths, as well as geolocations of the two groups, are different. In normal cases, channels 10-13 are four scans ahead of channels 1-9, and the swath width of channels 10-13 is about 50 km narrower than that of channels 1-9. Figure 3-5 show comparisons of GMI geometry and brightness temperatures between 37 GHz and 183 ± 3 GHz channels.

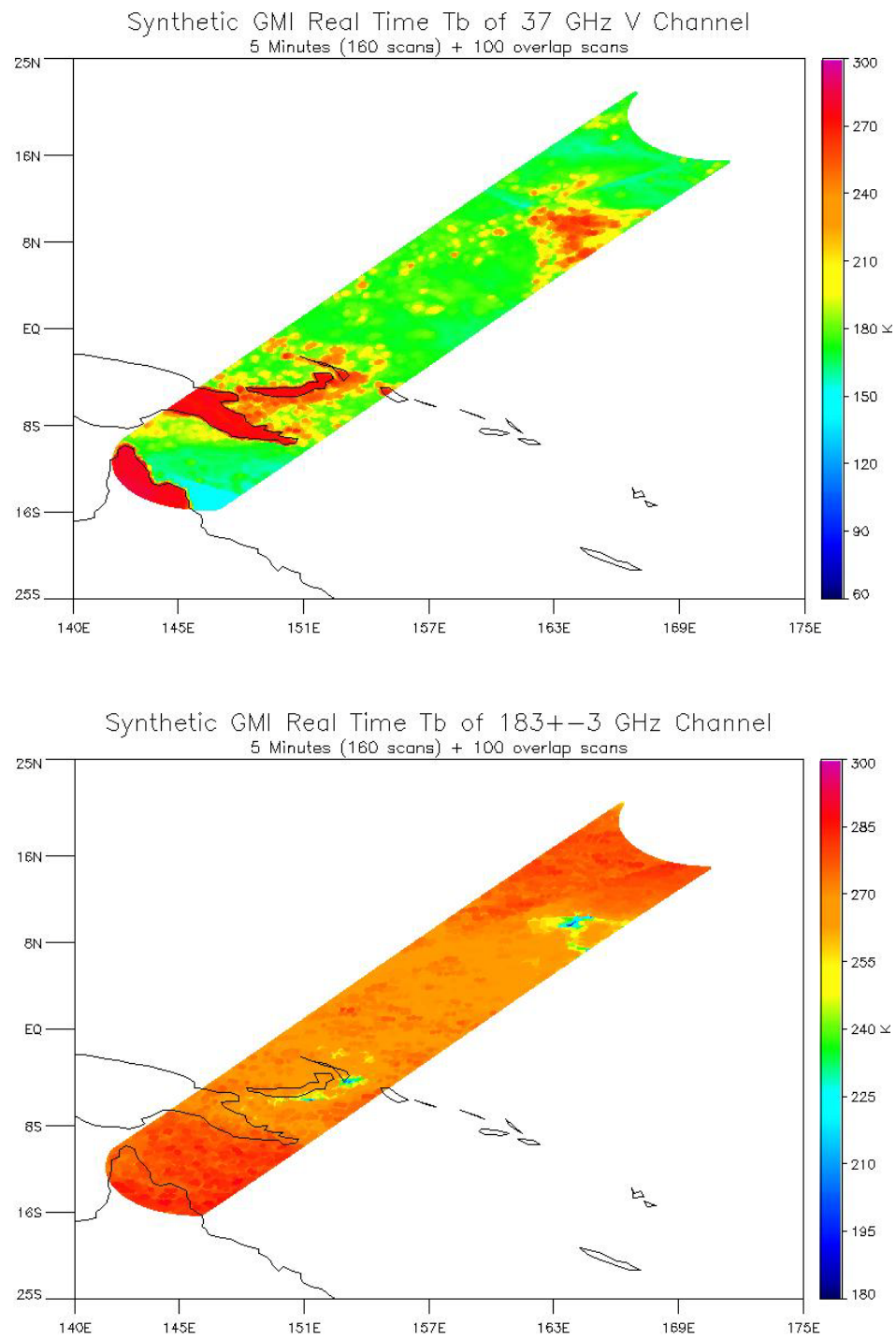


Figure 3-5. Simulated 5-Minute Section of 37 GHz Channel T_b (Upper)
and 18 ± 3 GHz T_b (Lower)

3.1.5 Noise Diodes and Four-Point Calibration

The noise diodes are implemented for channels 1-7. These noise diodes are turned on for every other scan such that additional calibration measurements are taken to perform four-point calibration to determine sensor non-linearity. Figure 3-6 is the schematic diagram of four-point calibration.

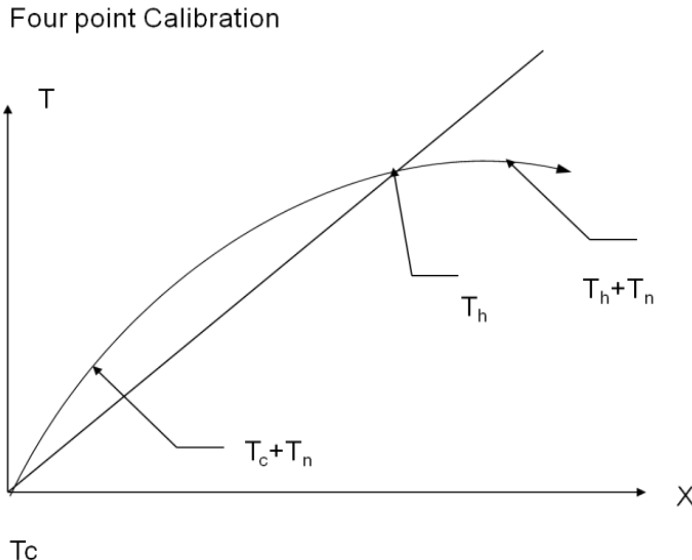


Figure 3-6. Schematic Diagram of GMI Four-Point Calibration

For cold load + noise diode measurement, the equation is:

$$T_{cn} = T_c + T_n = X_{cn} * T_h + (1-X_{cn}) * T_c - 4 * T_{nl} * X_{cn} * (1-X_{cn}) \quad (3.6)$$

Where:

T_n: Noise Diode Temperature

$$X_{cn} = (C_{cn} - C_c) / (C_h - C_c)$$

C_{cn}: Cold Load + Noise Diode Count

The equation is similar for hot load + noise diode measurement:

$$T_{hn} = T_h + T_n = X_{hn} * T_h + (1-X_{hn}) * T_c - 4 * T_{nl} * X_{hn} * (1-X_{hn}) \quad (3.7)$$

Where:

$$X_{hn} = (C_{hn} - C_c) / (C_h - C_c)$$

C_{hn}: Hot Load + Noise Diode Count

The non-linearity can be derived from Equations (3.6) and (3.7):

$$T_{nl} = (T_h - T_c) / 4 * (X_{hn} - X_{cn} - 1) / (X_{hn} (1 - X_{hn}) - X_{cn} (1 - X_{cn})) \quad (3.8)$$

3.1.6 Back-up Calibration Algorithm

Using C_{cn} and T_{cn} , a hot load backup algorithm may be derived in case there is no hot load information:

$$T_a = X_b * T_{cn} + (1-X_b) * T_c - 4 * T_{nl} * X_b * (1-X_b) \quad (3.9)$$

Where:

$$X_b = (C - C_c) / (C_{cn} - C_c)$$

3.2 ANTENNA PATTERN CORRECTION

Corrections of the calibrated antenna temperatures are performed following the radiometric calibration in order to transform calibrated antenna temperature to brightness temperature. The antenna temperature of each pixel is corrected for the co-polarization, cross-polarization, and spillover effects of the antenna. The brightness temperature T_b will be derived from Equation (3.10):

$$T_b = C_n T_a + D_n T_a^* + E_n \quad (3.10)$$

T_a^* : Antenna temperature of cross-polarized channel of the T_a

C_n , D_n , and E_n : APC coefficients are derived from in-flight simulation using radiative transfer models with antenna patterns as well as a global database. The APC coefficients will be provided by Ball Aerospace or the GPM Intercalibration Working Group (X-CAL).

INPUT, OUTPUT, AND ALGORITHM FLOW CHART

The input files for calibration include L1A, ephemeris files from GeoTK, and external tuning files. The L1A is an assembly of spacecraft (SC) and housekeeping (HK) telemetry files, as well as GMI ancillary files for a designated time period. For regular data, it will be an orbit plus 50 scans overlap before and after the orbit. For real time, it will be a segment of 5 minutes plus 50 scans overlap before and after the section. L1B unpacks the SC and HK packets to retrieve designated Earth observation and calibration data. The tuning file will include all externally determined data, such as APC coefficients and hot load PRT weights. The key input parameters are listed in Table 3-1.

The key output parameters include geolocated and calibrated T_a and T_b , as well as parameters required by higher level algorithms such as incidence angle, Sun glint angle, etc. The details of output parameters are presented in separate documents: GMI Base File Specification, and GMI L1B File Specification.

The flow diagram of GMI calibration is displayed in Figure 3-7.

Table 3-1. Key Input Parameters

Parameter	Dimension	Unit	Description	Source
Noise Diode Indicator	n_{scans}		0=Noise Diode Off 1=Noise Diode On	SC Packets
Earth View Count	$n_{chan}, n_{scans}, n_{pixels}$	Counts	All Scans	SC Packets
Hot Load Count	$n_{chan}, n_{scans}, n_{hsample}$	Counts	Every Other Scan	SC Packets
Cold Load Count	$n_{chan}, n_{scans}, n_{csample}$	Counts	Every Other Scan	SC Packets
Hot Load + Noise Diode Count	$n_{chan}, n_{scans}, n_{hsample}$	Counts	Every Other Scan	SC Packets
Cold Load + Noise Diode Count	$n_{chan}, n_{scans}, n_{csample}$	Counts	Every Other Scan	SC Packets
Hot Load Temperature	$11, n_{scans}$	Kelvin	All Scans	HK Packets
Cold Sky Temperature	n_{chan}, n_{scans}	Kelvin	All Scans	Tuning Data
Hot Load PRT Weights	$11, n_{chan}, n_{hsample}$		All Scans	Tuning Data
APC Coefficients	3		All Scans	Tuning Data
Non-Linearity	n_{chan}	Kelvin	All Scans	Tuning Data

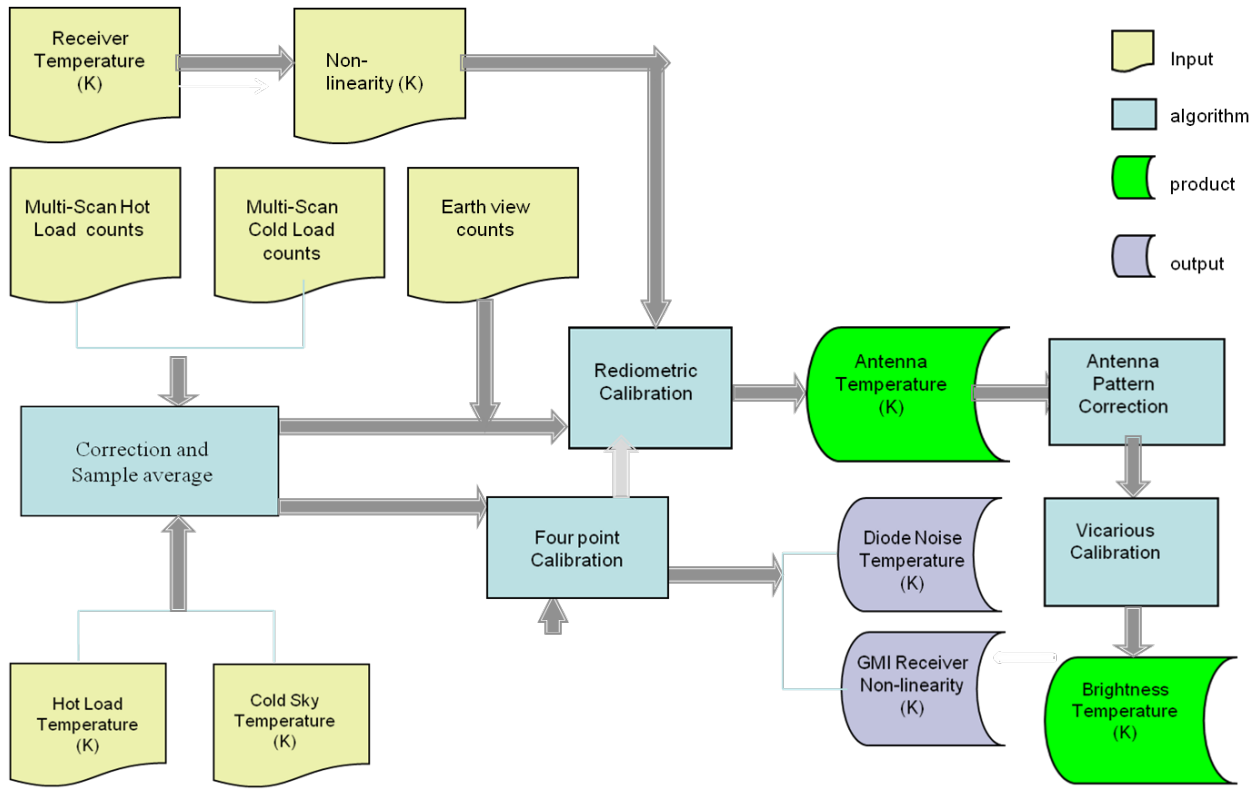


Figure 3-7. Flow Chart of GMI L1B Calibration Process

3.3 PRE-LAUNCH SIMULATION AND SYNTHETIC L1B DATA

The pre-launch simulation will utilize radiation models to generate a synthetic GMI T_b data set for the use of testing for higher level algorithms. The objective is to provide coincident antenna temperatures and brightness temperatures for 13 GMI channels. The data format shall meet the GMI L1B file specification, and the data shall contain various cloud and precipitation features and can be used to test PPS flow from GMI L1 to L4 before launch of the satellite.

The simulation will also generate statistical comparisons of T_b s between existing sensors (TMI, AMSR-E, AMSU-B, etc.) and GMI for similar channels. Table 3-2 shows the comparison of channel characteristics between GMI and existing satellite sensors.

A flow diagram of the derivation of synthetic GMI T_b is shown in Figure 3-8. Figure 3-9 shows the T_b relationship between GMI 36.5 GHz and TMI 37.0 GHz channels and between GMI 89 GHz channel and TMI 85.5 GHz channels.

Table 3-2. Comparison of Channel Characteristics Between GMI and Existing Satellite Sensors

GMI	10.65 V low	10.65 H low	18.7 V low	18.7 H low	23.8 V low	36.5 V low	36.5 H low	89.0 V high	89.0 H high	165.5 V high	165.5 H high	183 ± 3 high	183 ± 7 high
TMI	10.65 V low	10.65 H low	19.35 V low	19.35 H low	21.3 V low	37.0 V low	37.0 H low	85.5 V high	85.5 H high				
AMSRE	10.65 V low	10.65 H low	18.7 V low	18.7 H low	23.8 V low	36.5 V low	36.5 H low	89.0 V high	89.0 H high				
SSMIS			19.35 V low	19.35 H low	22.23 V low	37.0 V low	37.0 H low	91.66 V high	91.66 H high		150 H high	183 ± 3 high	183 ± 7 high
AMSUB								89.0 V low		150.0 V low		183 ± 3 low	183 ± 7 low
GMI Channel #	1	2	3	4	5	6	7	8	9	10	11	12	13

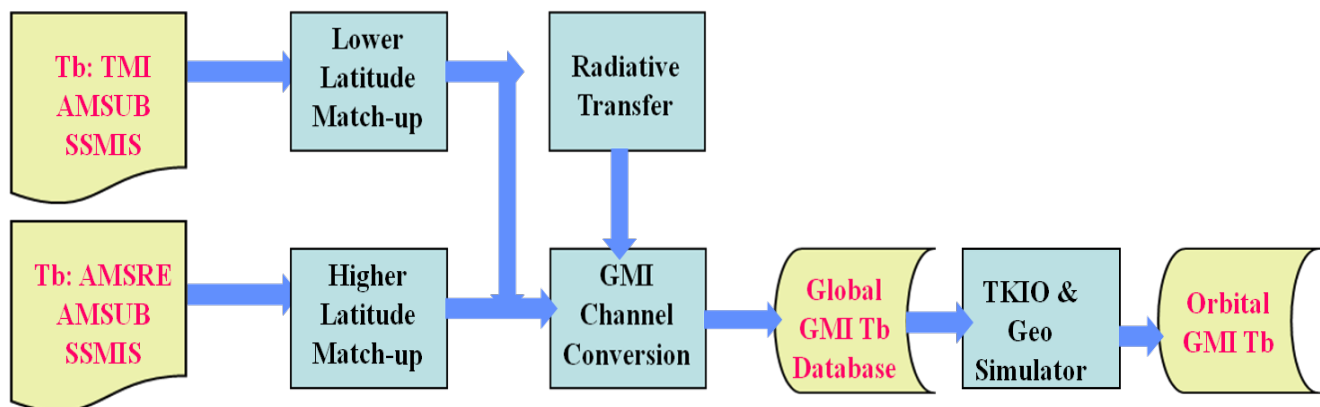


Figure 3-8. Flow Diagram of Derivation of Synthetic GMI T_b

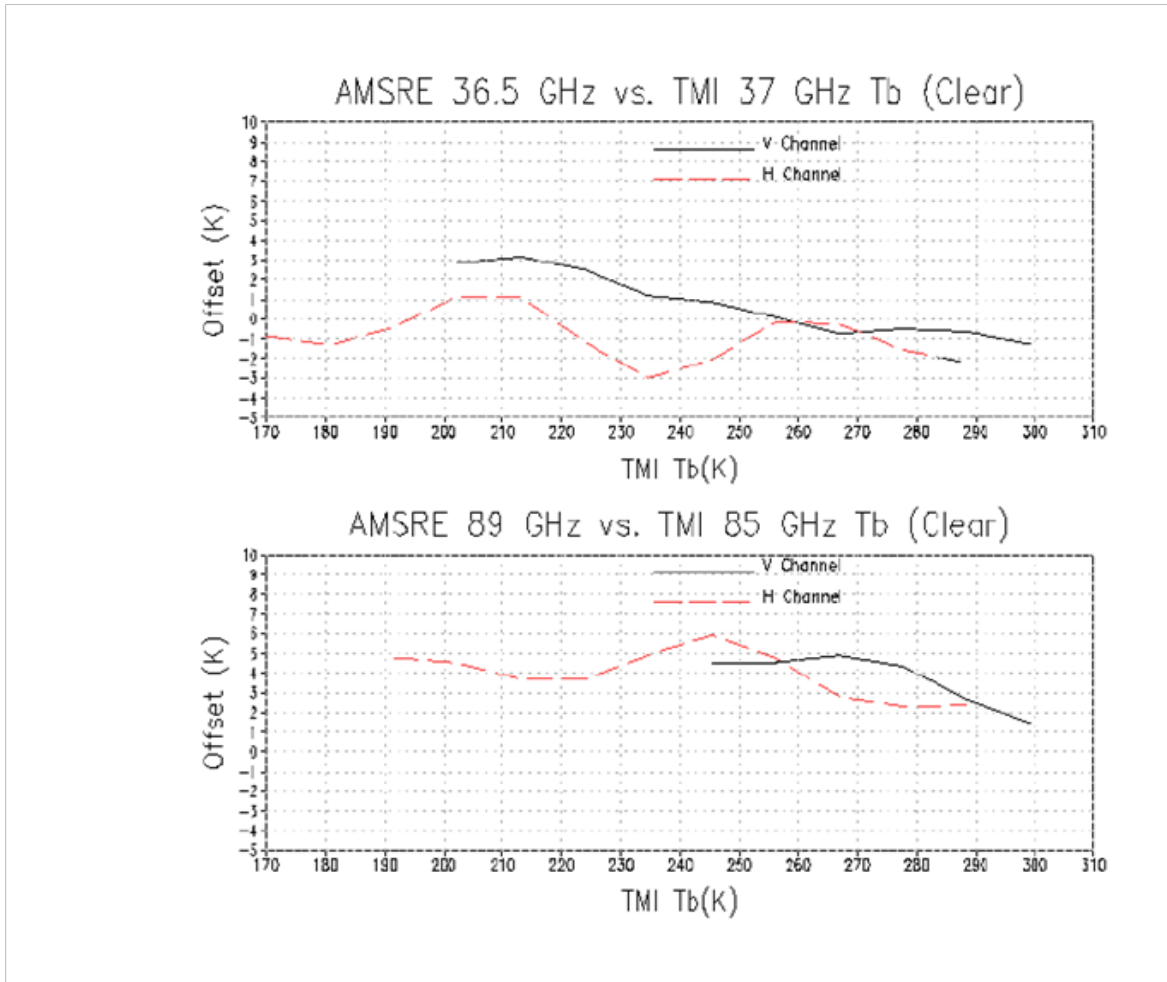


Figure 3-9. T_b Relationships Between GMI 36.5 GHz and TMI 37.0 GHz Channels and Between GMI 89 GHz and TMI 85.5 GHz Channels

Figure 3-10 and Figure 3-11 show examples of global and orbital synthetic T_b data, and Figure 3-12 is the flow diagram of using synthetic T_b data to test the processing flow.

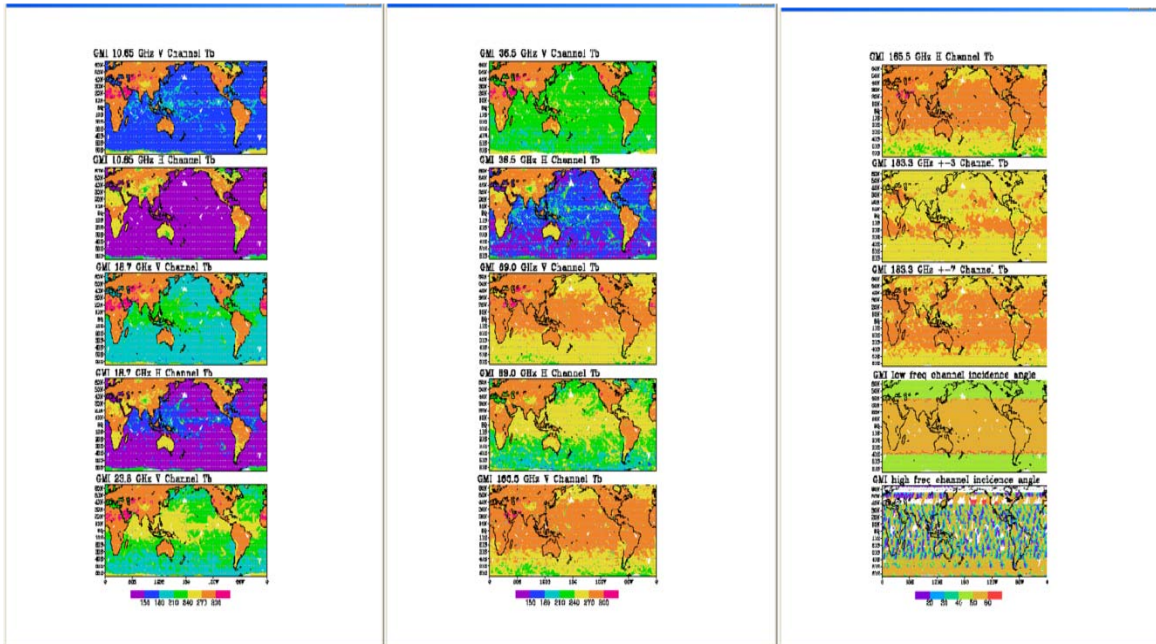


Figure 3-10. Global GMI T_b Database for Northern Summer

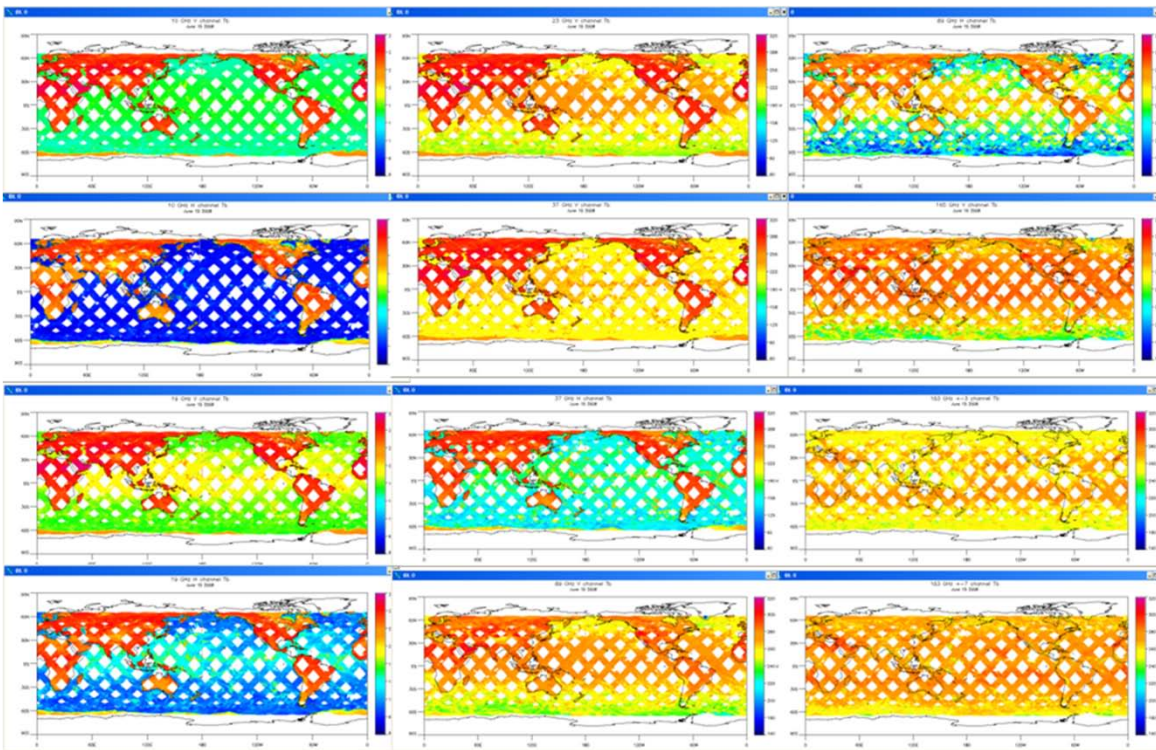


Figure 3-11. Synthetic Orbital GMI T_b for June 15, 2008

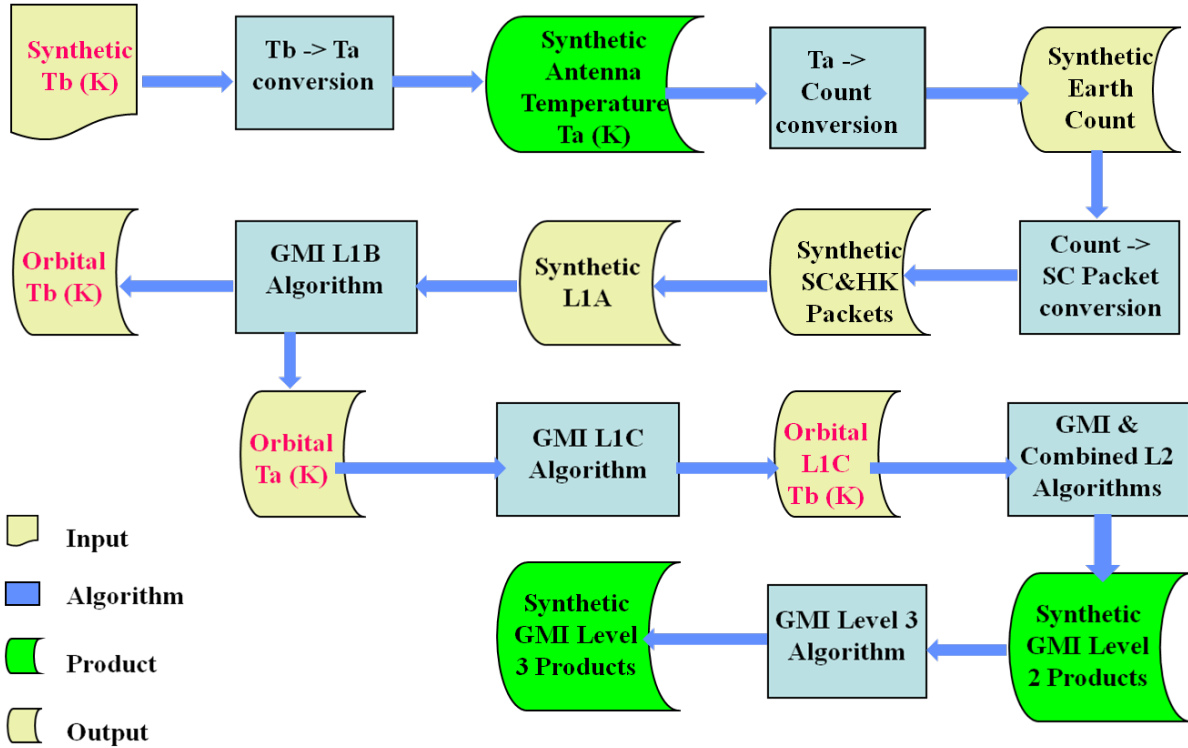


Figure 3-12. Flow Diagram of Synthetic Data Processing

3.4 POST-LAUNCH VALIDATION AND CALIBRATION

The post-launch validation and calibration employ the following aspects:

- Pointing error check.
- Along-scan correction.
- Inter-comparison and statistical analysis.
- Deep-space satellite maneuver.

3.4.1 Pointing Error Check

Analysis and correction of sensor pointing errors is the first step in the post-launch calibration/validation plan. Those errors include misspecification of nadir angle, azimuth angle, spacecraft attitude, or time of the measurement. Different types of pointing errors have been observed in other instruments, and each instrument had its own specific problem. TMI, AMSR-E, and WindSat exhibited misspecifications of the spacecraft attitude; in WindSat, there were in addition misspecifications of the azimuth offset; and in SSMIS, the value of one of the nadir angles was incorrect. It is difficult to specify the pointing geometry pre-launch to the necessary degree of accuracy.

The basic method for checking the pointing accuracy and correcting potential errors is to calculate high-resolution ($1/4^\circ$ or higher) global maps of average antenna temperature measurements for both the ascending and the descending swath, and then plot the map of the differences of both. Pointing errors will cause contours along coastlines and large rivers on the

map. For most cases, it is enough to use 1 to 3 months of data for the averaging. The misspecification is then found and corrected by trial and error.

3.4.2 Along-Scan Correction

The second step in the post-launch calibration/validation plan is the analysis of T_a (measured) minus T_a (RTM) as a function of the along-scan position or Earth sample. This is especially important for a calibration/validation shortly after launch where only a relatively small (1-month to 3-month) data set is available. Generally it is safer to work on the T_a level rather than on the T_b level.

In this step, systematic deviation from a constant value and the variation of this deviation over the scan are investigated. The standard deviation of T_a (measured) minus T_a (RTM) as a function of scan position also must be analyzed.

The absolute calibration is an on-orbit readjustment of the cross-polarization and spillover parameters using T_b s that were calculated from the RTM and T_a s that were measured by the radiometer.

The absolute calibration is necessary because accurate pre-launch measurements of the antenna patterns are very difficult, especially for the back lobes. This, in turn, makes it very difficult to accurately determine the spillover value before launch. Another purpose of the absolute calibration is to remove any residual biases within the calibration procedure.

It should be noted that the absolute calibration absorbs some other residual biases that have not been removed yet. In many cases, the effects of those biases are indistinguishable and therefore get absorbed in the same way.

3.4.3 Inter-Comparison and Statistical Analysis

The inter-comparison compares results between the GMI observations and collocated observations taken by other instruments.

Statistical analysis is used to find systematic errors. This method requires only GMI observations. Typically, GMI is a conically scanning radiometer, maintaining a nearly constant Earth incidence angle throughout the scan. In principle, the measurement characteristics of the sensor should be completely independent of scan position. However, in practice, problems such as spacecraft attitude errors, obstructions in field of view, and side lobes detecting the spacecraft may result in systematic errors that are a function of scan position. Given enough observations, the along-scan error can be determined by making the assumption that the effect of weather and surface features is, on average, the same at all scan positions.

3.4.4 Deep-Space Maneuver

Analysis of the GMI observations during orbit maneuvers in which the GMI main reflector observes cold space may provide good indicators of GMI calibration quality.

4.0 L1B DATA PRODUCT

4.1 LEVEL 1B PROCESSING

4.1.1 Satellite Maneuver

The GPM satellite will occasionally perform special maneuvers. These maneuvers take place to support the calibration and maintenance of the various instruments on board. The GPM instruments will continue collecting data during satellite maneuvers, although the collected data may not always have scientific value. It is left to higher level processing to decide whether or not the collected, geolocated, and calibrated data are useful. Annotations are made in the data QA fields to indicate that maneuvers were in progress while the associated data were collected. The geolocation quality flag will record when special maneuvers are taking place.

4.1.2 GMI L1B Processing

L1B processing processes the GMI L1B algorithm. The input of L1B processing is GMI L1A and ephemeris data. The L1A data include L0 science packet (after de-segmentation) and HK packet data, as well as geolocation information from the global positioning system (GPS). The processing includes geolocation and calibration of GMI data, and QA processing. L1B GMI processing is composed of activation, execution, and termination.

4.1.2.1 Activation

The scheduler spawns L1BGMImain as an autonomous process upon the availability of a GMI Level 1A granule and ephemeris from the Geolocation Toolkit. The scheduler passes it several parameters as follows:

- Granule ID of the L1A granule that is the input data to the L1B processing.
- Ephemeris ID that is the input data to the L1B processing.
- Granule ID of the L1B granule that is the output file.

4.1.2.2 Execution

The flow chart for executing the main program is shown in Figure 4-1.

First, module L1BGMImain opens the input L1A granule and ephemeris files, as well as the output L1B granule files. The log files are also opened.

Next, L1BGMImain reads the granule header from the L1A granule. L1BGMImain then initializes the geolocation processing that reads the model parameters file and carries out various initial calculations required for processing geolocation.

Then L1BGMImain calls the function L1BdoScans, the driver routine that manages the scan-by-scan processing. It determines the number of science packets in the granule and loops through this number. For each packet, routines are called to unpack, geolocate, calibrate, perform QA, collect metadata, and output the scan. L1BdoScans also reads missing data unit list (MDUL) packets and calls geolocation, metadata collection, and outputting routines for each missing scan.

Upon completion of L1BdoScans, L1BGMImain calls the function L1BfinalizeMetadata, which takes the L1Bmetadata structure and calculates the final values for all metadata items and outputs the metadata to the L1B granule.

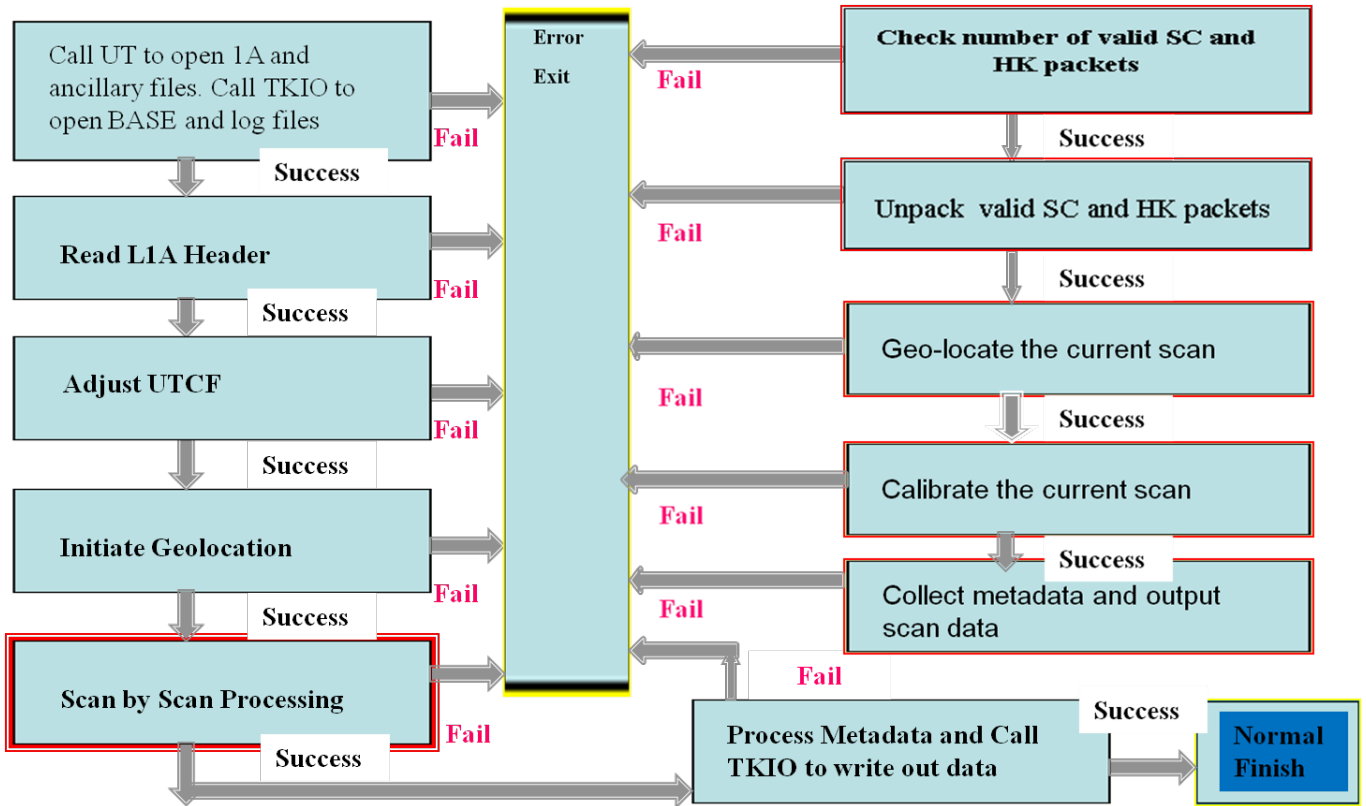


Figure 4-1. Flow Chart for Executing the L1B Main Program and Scan-by-Scan Processing

4.1.2.3 Termination

When L1BGMImain finishes execution, successfully or otherwise, it passes a return code to the scheduler and stops (ceasing to exist as a spawned process). The return code tells the scheduler the reason for termination. The following return states are defined:

- Problem reading input (i.e., no L1B created).
- Problem creating output (i.e., no L1B created).
- Fatal anomaly interrupted processing (i.e., partial L1B created).
- Normal termination (i.e., L1B created).

4.2 DATA STRUCTURE

The format of the GMI L1B product is Hierarchical Data Format, Version 5 (HDF5). PPS has developed Interactive Data Language (IDL) tools to view the data and both C and Fortran programs to help users to read the data. The details of the metadata and data structure are in the PPS L1 software design specification (SDS) document.

4.2.1 Metadata

The GMI L1B software generates much information that eventually becomes metadata. Throughout the software execution, the information is kept in local data structures. Near the conclusion of each executable's life, calls are made to the Toolkit function, and information from the local data structures is recorded as metadata.

4.2.2 Structure

Key Level 1B structures will be presented in the GMI L1B File Specification.

5.0 REFERENCES

- Bilanow, S., 2010: PPS GeoTK ATBD.
- Bilanow, S., 2010: PPS Geolocation Toolkit Architecture and Design Specification.
- Stout, J. M., 2010: PPS File Specification.
- Wentz, F. J., and M. Thomas, 2008: GMI Calibration ATBD.

APPENDIX A. ACRONYMS AND ABBREVIATIONS

AMSR	Advanced Microwave Scanning Radiometer
AMSR-E	AMSR Earth Observing System
AMSU-B	Advanced Microwave Sounding Unit-B
APC	Antenna Pattern Correction
ATBD	Algorithm Theoretical Basis Document
CSR	Cold Sky Reflector
GeoTK	Geolocation Toolkit
GHz	GigaHertz
GMI	GPM Microwave Imager
GPM	Global Precipitation Measurement
GPS	Global Positioning System
GSFC	Goddard Space Flight Center
HDF5	Hierarchical Data Format, Version 5
HK	Housekeeping
ID	Identification
IDL	Interactive Data Language
L1A	Level 1A (Algorithm)
L1B	Level 1B (Algorithm)
MDUL	Missing Data Unit List
NASA	National Aeronautics and Space Administration
PDR	Preliminary Design Review
PPS	Precipitation Processing System
PRT	Platinum Resistance Thermometer
QA	Quality Assurance
RSS	Remote Sensing System
RTM	Radiative Transfer Model
SC	Spacecraft
SDS	Software Design Specification
SSM/I	Special Sensor for Microwave Imager
SSMIS	Special Sensor for Microwave Imager/Sounder
T _a	Antenna Temperatures
T _b	Brightness Temperatures
TBD	To Be Determined
TMI	TRMM Microwave Imager
TRMM	Tropical Rainfall Measuring Mission
X-CAL	GPM Intercalibration Working Group